Implementation of a Combination Planar and Spherical Near-Field Antenna Measurement System using an Industrial 6-Axis Robot

John Hatzis, Patrick Pelland, Greg Hindman
NSI-MI Technologies, Torrance, CA, USA
jhatzis@nsi-mi.com, ppelland@nsi-mi.com, ghindman@nsi-mi.com

***Abstract*— Near-field antenna test systems are typically designed to optimize measurement results for a specific type of antenna. The measurement system is selected and sized based on the antenna aperture dimensions, directivity, weight and operating frequency, among other parameters. These factors are used to select either a planar, cylindrical, or spherical near-field test system for the given antenna test requirements. Antennas with different characteristics may not be compatible with the selected range and often require costly upgrades to the existing range or a different range altogether. One solution to test a wide variety of antenna types is a combination planar-cylindrical-spherical (PCS) test system. These systems usually require some level of facility re-configuration and present drawbacks when switching between the various modes of operation.**

The adaptation of a six-axis robotic test system is an attractive solution in these situations, as the system's flexibility allows for rapid reconfiguration that is inherent to the system. This allows the user to select the optimal test solution for the antenna under test with little effort. This paper presents the performance of a six-axis robotic near-field measurement system showing near-field modes of operation and the system's performance in antenna measurements when compared to a traditional spherical near-field range.

Index Terms— robot, robotic, near-field, planar, spherical

I. INTRODUCTION

Near-field antenna test systems are typically selected by the type of antenna that will primarily be tested in the system. Such systems are principally constructed of spherical, planar and cylindrical configurations. Each configuration is drastically different from the other.

Spherical near-field (SNF) antenna test systems allow for accurate characterization of an antenna's radiation pattern over a full sphere by minimizing the truncation effects and allowing for effective characterization of side lobes and back lobes. This is particularly attractive for testing antennas with low directivity. Additionally, SNF measurements are ideal for testing low gain antennas when placing the antenna under test (AUT) in the far-field is not practical due to size or frequency limitations. However, spherical near-field systems require very precise alignment for accurate measurements and often require larger anechoic chambers compared to other configurations.

Planar near-field (PNF) systems are widely used for testing directive antennas but are not suitable for antennas with low directivity. Such systems exist in horizontal and vertical configurations. However, the inherent configuration of planar systems limits the angular extent of the electric field that can be measured. Side lobes far from the main lobe are not measured and as such, the maximum far-field angle that can be measured is limited.

Users who require testing a wide variety of antennas typically resort to acquiring multiple configurations, which represents a significant capital investment. A six-axis industrial robot (as depicted in Figure 1) supports testing a variety of antennas under different configurations using one system. Such a system has recently been developed to operate in spherical near-field [1-5] and in planar near-field modes.

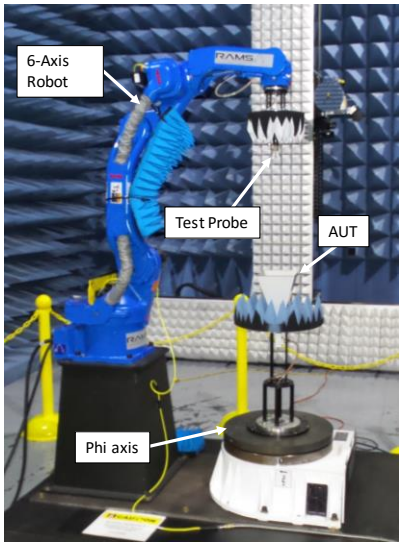

Figure 1. Robotic scanner in a θ/φ SNF configuration

This paper will outline the planar and spherical configurations possible with a robotic antenna measurement system (RAMS), demonstrate the alignment accuracy that has been achieved, and analyze antenna patterns measured.

II. ALIGNMENT IN NEAR-FIELD TEST CONFIGURATIONS

Near-field systems require precise alignment and positional accuracy for accurate antenna characterization. These requirements are different for the various measurement configurations.

A. A. SNF Measurement Geometries

Spherical near-field systems exist in a variety of configurations to acquire data on a spherical surface. Two of the most common types of SNF test systems are ϕ-over-θ (ϕ/θ) type systems and θ-over-ϕ (θ/ϕ) systems.

ϕ/θ are the most common SNF configurations, in which two rotary stages are joined by a common structure. The stage mounted on the floor forms the θ-axis of rotation whereas the upper stage on which the AUT is mounted forms the ϕ-axis. The pol axis is typically mounted on a separate structure. In this configuration, the AUT is typically in constant rotation on the φ axis and stepped in the θ axis, to form a complete measurement sphere. This can be a disadvantage for delicate antennas due to the constantly changing gravity vector [6].

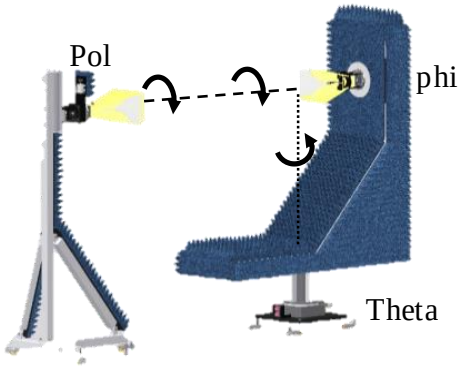

Figure 2. Diagram showing a ϕ/θ SNF configuration

θ/ϕ SNF systems were developed to limit the motion of the AUT to keep the gravity vector direction unchanged. This configuration is essentially a rotated ϕ/θ system. However, in the ϕ/θ system the pol and θ axes are connected, whereas in the θ/ϕ configuration the θ and ϕ axes are disconnected, requiring precise alignment. The lower stage forms the ϕ axis while the upper stage forms the θ axis [6].

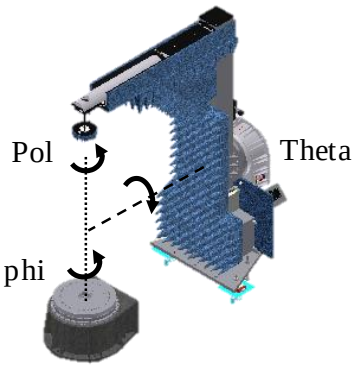

Figure 3. Diagram showing a θ/ϕ SNF configuration

SNF antenna measurements require both amplitude and phase information to be collected over the measurement sphere in both polarizations for transformation to the far-field. Data is typically acquired in two scan geometries:

$$-180° \le \theta \le +180°,\ 0° \le \phi \le 180°$$
$$0° \le \theta \le +180°,\ 0° \le \phi \le 360°$$

Both of these geometries acquire a complete sphere. However, allowing both axes to rotate a full revolution will result in a redundant sphere being measured, which offers several advantages. These advantages are outlined elsewhere [7].

B. SNF Sensitivity to Alignment

Proper alignment of the axes of motion is critical in order for measurements to result in good far-field patterns. In both θ/ϕ and ϕ/θ configurations the following alignment conditions and structural requirements must be met [6,8]:

1. All axes must intersect and in particular the probe axis must be co-linear with the ϕ axis at θ=0°
2. The θ and ϕ axes must be orthogonal
3. All stages must not exhibit coning or runout
4. The support structure has to be rigid

Alignment is verified using a laser tracker or similar means. For traditional spherical scanners, alignment – and in particular non-intersection of the axes – involves physically and iteratively manipulating the rotary stages. This alignment becomes particularly cumbersome when performed with the AUT and probe mounted on their respective positioners. A robotic system, on the other hand, can be realigned by adjusting the robot to the desired acquisition grid with great ease and accuracy.

C. PNF Implementations

A planar near-field scanner is composed of two stages that position a probe in Cartesian coordinates. The objective is to create a plane that is perfectly flat. Typically, a polarization positioner is included, as is a probe translation stage. The latter is used to offset the probe and for correcting imperfections in the scan plane due to the scanner structure.

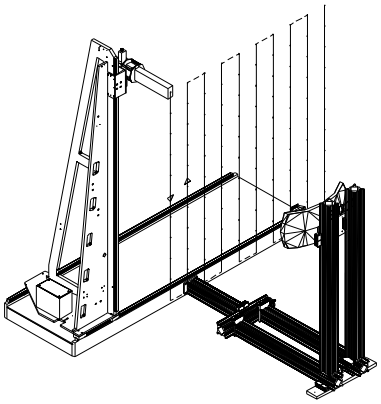

Figure 4. Diagram showing a typical vertical PNF configuration

Planar systems have a limited span, and as such suffer from truncation effects. Therefore, it is impractical to measure side

lobes outside of a roughly +/- 70° region and these systems are limited to testing directive antennas. Since the geometry is not fixed, the AUT can be placed close to the scan plane, resulting in improved signal to noise ratio (SNR) in most tests. The typical positional accuracy required is λ/50. [1,6]

III. Implementation of a Robotic Near-Field Scanner

NSI-MI Technologies recently developed a multi-purpose scanner based on an industrial 6-axis robot as a multi-configuration near-field scanner expanding on previous work [3]. The system is composed of six rotary axes embedded in the robot that are coupled with an external axis on which the AUT is mounted.

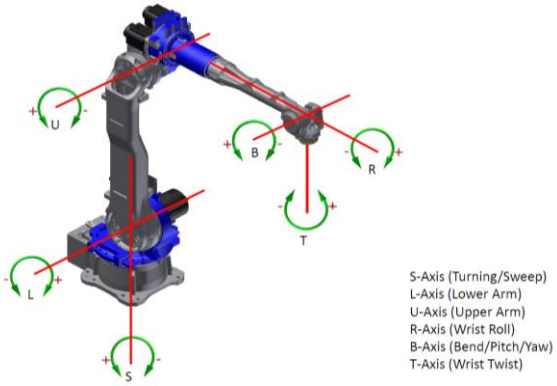

Figure 5. Illustration of the axes of a six-axis industrial robot

The six rotational axes are combined in motion to result in an arbitrary position within the mechanical reach of the robot.

A. *Limitations of Robotic System*

While the robotic system allows most any scan geometry, the extents of each geometry are not constant as parameters such as AUT size, probe length, or probe to AUT distance are varied. In such a system, the size of the AUT and lowest operating frequency define the system limitations.

Consider the θ/ϕ SNF configuration depicted in Fig. 6. Here the robot is used to measure a 1 m diameter AUT at 4 GHz using a WR-187 open-ended waveguide probe. The surface of the robot arm cannot be closer than the sum of the probe length, 3 λ offset to the AUT, and the radius of the AUT from the center of the inscribed circle. In this case, the maximum θ angle that is achieved is ±128°. Varying the total tool length by using a shorter probe or reducing the probe to AUT distance results in a maximum θ angle of ±136°. This is depicted in Fig. 7. This limitation is due to the B-axis of the robot reaching its mechanical limits. Practically, this means that AUTs requiring longer total tool lengths, i.e. operating at lower frequencies, will need to be directive to minimize truncation effects.

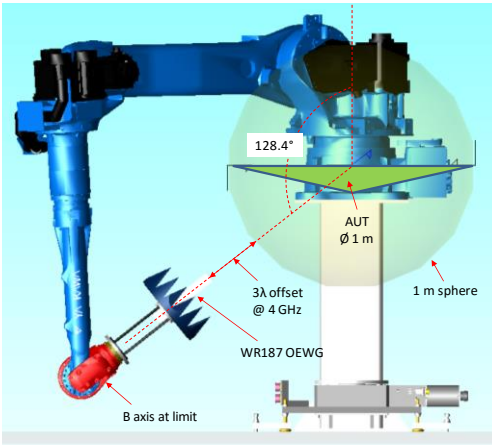

Figure 6. Limitation of θ axis in a φ/θ SNF configuration

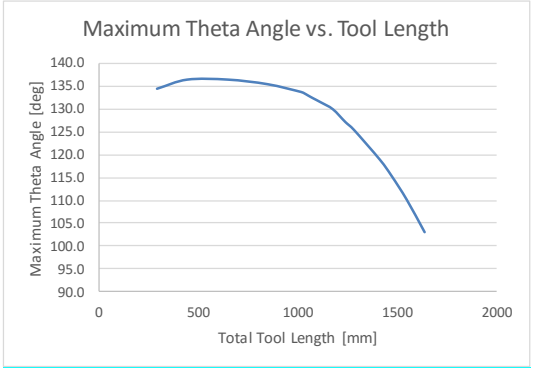

Figure 7. Limitation of max θ angle as a function of tool length

Similar limitations hold when the robot is being used in a planar near-field configuration. Again, considering a robotic system outfitted with a WR-187 open-ended waveguide probe, the maximum square plane that the robot can describe varies greatly with the scan plane position relative to the robot mounting height.

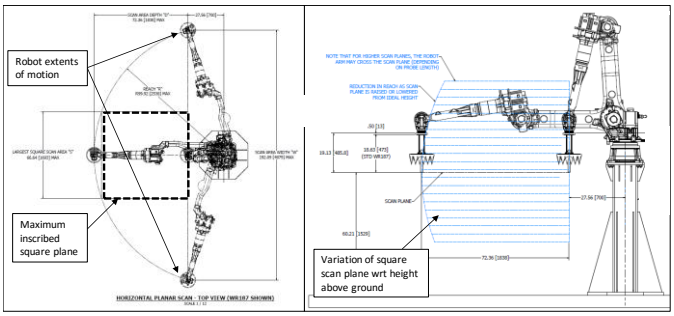

Figure 8. Robotic PNF inscribing a horizontal plane

The extents of motion of the robot when inscribing a horizontal scan plane are shown in Fig. 8. In order for the scan plane to be maximized, the AUT must be placed at an optimum height above ground. This parameter is a critical design criterion when determining the height of the robot pedestal, which is defined by the characteristics of the AUT. The maximum size square plane with respect to height above ground is shown in Fig. 9.

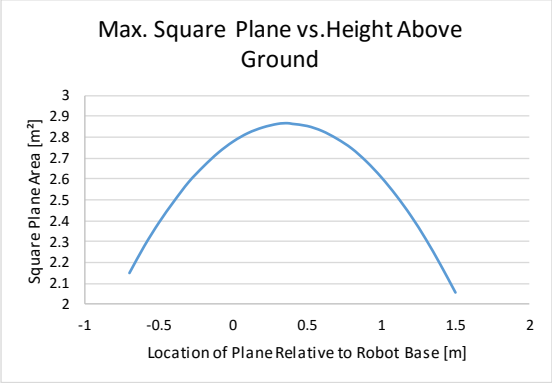

Figure 9. Variation of scan plane as function of height above ground

Similar limitations exist in other modes of operation, such as vertical planar and tilted planar modes, but these are not elaborated on here.

B. Mechanical Accuracy and Alignment

The robotic system was aligned, and its mechanical accuracy was investigated using a laser tracker. First, the robotic system was aligned as a θ/ϕ configuration. The probe used was a WR-187 open-ended waveguide, and the AUT used was an WR-187 standard gain horn mounted on a 500 mm rotation stage as shown in Fig. 10.

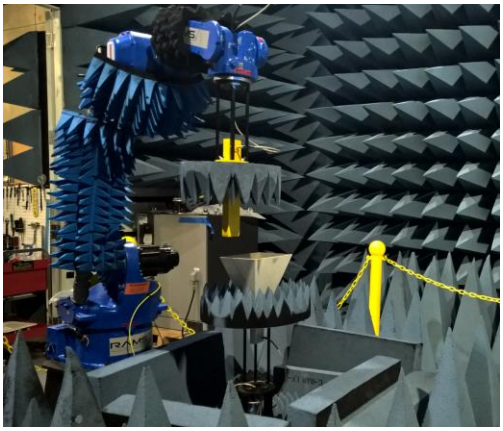

Figure 10. Robotic scanner in θ/ ϕ SNF and horizontal PNF configuration

The intersection error of the ϕ and θ axes was established by comparing the origins of the circles inscribed by the ϕ stage and θ stages. In traditional θ/ ϕ systems, the ϕ or pol axes would have to be mechanically repositioned during the alignment process. With a large 500 mm ϕ stage such as the one used in this case, precise alignment becomes extremely difficult. The robotic system was easily aligned by modifying the origin of motion of the robot so that the center of rotation of the θ axis intersected the ϕ axis. The θ/ϕ orthogonality errors are due to the circle inscribed by the RAMS θ axis having an "out of plane error", which can be corrected by implementing a correction of y position as a function of θ (variables are depicted in Fig. 11).

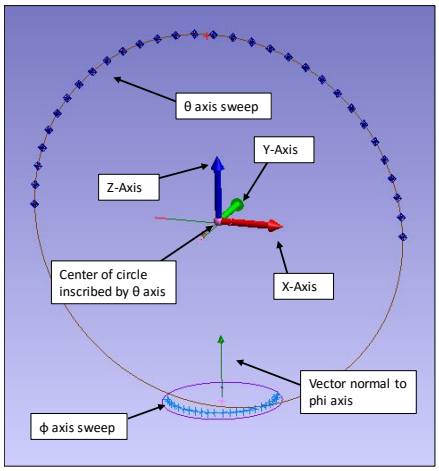

Figure 11. θ/φ configuration as measured with laser tracker

The θ axis angular position was also characterized and this is depicted below in Fig. 12. The measured values were employed as a correction grid and applied in order to minimize the angular error. The net result of this is also shown in Fig. 12. No radial correction was applied; however, it is planned to develop this capability and investigate the effects in the future.

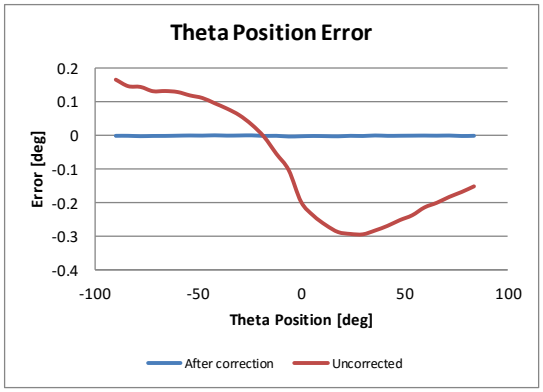

Figure 12. Angular θ error before and after correction was applied

Following alignment, the robotic system achieved the following results:

TABLE I. RAMS ALIGNMENT

Axis intersection error	0.068 mm
θ/φ orthogonality error	0.196°
θ error	< 0.001° RMS
Radius error	0.362 mm RMS
θ axis deviation from plane	0.435 mm RMS

The alignment results show that the robotic system has excellent intersection error, and θ error, but has a large radius error and planarity error of the circle inscribed by the θ axis. The nature of the robot allows for unconstrained motion, so better characterization is needed to improve the θ planarity and to correct for radial error. The ϕ planarity reflects a stage independent to the robot.

The RAMS was also characterized in horizontal PNF mode. The uncorrected performance was measured and then a correction grid was implemented. The planarity was corrected to 0.016 mm RMS, which is excellent and consistent with robot repeatability seen previously [1,5]. The planarity is also similar to that of traditional PNF systems The results are shown below:

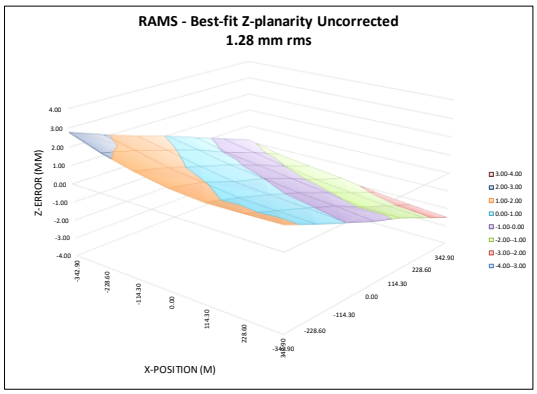

Figure 13. Uncorrected z-axis planarity – 1.280 mm RMS

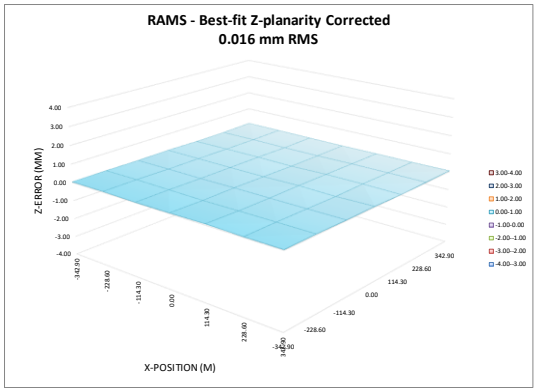

Figure 14. Corrected z-axis planarity – 0.016 mm RMS

IV. ANTENNA MEASUREMENTS USING ROBOTIC SCANNER

As an initial test case, the RAMS system was used to measure a WR-187 standard gain horn using a Panther RF subsystem. The plots below show preliminary comparisons between measurements taken on a traditional θ/ϕ SNF system using a PNA-based RF subsystem (in a different chamber) using pattern subtraction [8,9]. In addition, repeatability measurements were taken to assess the effects of random errors. Comparisons between the results of the SNF and PNF configurations of RAMS are also shown.

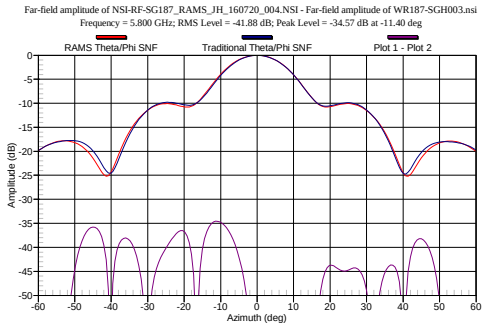

Figure 15. Azimuth cut comparison of RAMS and traditional θ/ϕ SNF
Freq.: 5.80 GHz, EMPL: -41.88 dB

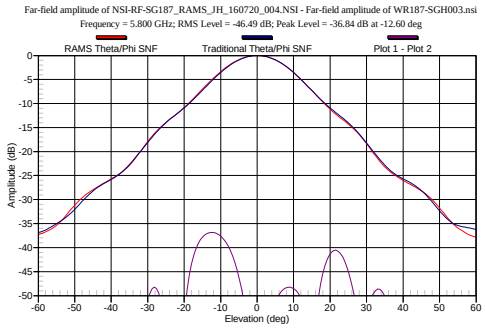

Figure 16. Elevation cut comparison of RAMS and traditional θ/ϕ SNF
Freq.: 5.80 GHz, EMPL: -46.49 dB RMS

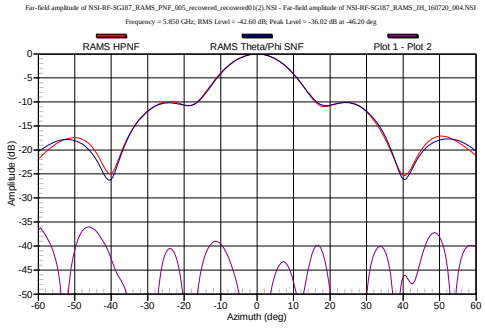

Figure 17. Azimuth cut comparison of RAMS PNF and SNF
Freq.: 5.85 GHz, EMPL: -42.60 dB RMS

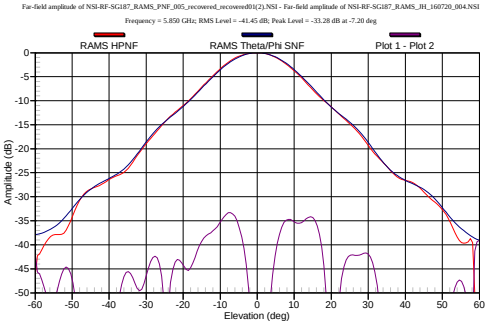

Figure 18. Elevation cut comparison of RAMS PNF and SNF
Freq.: 5.85 GHz, EMPL: -41.45 dB RMS

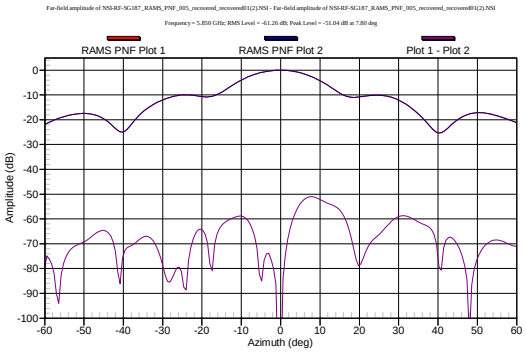

Figure 19. Azimuth cut repeatability comparison PNF RAMS Freq.: 5.85 GHz, EMPL: -61.26 dB RMS

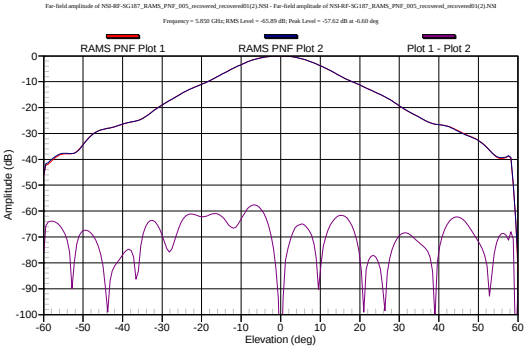

Figure 20. Elevation cut repeatability comparison PNF RAMS Freq.: 5.85 GHz, EMPL: -65.89 dB RMS

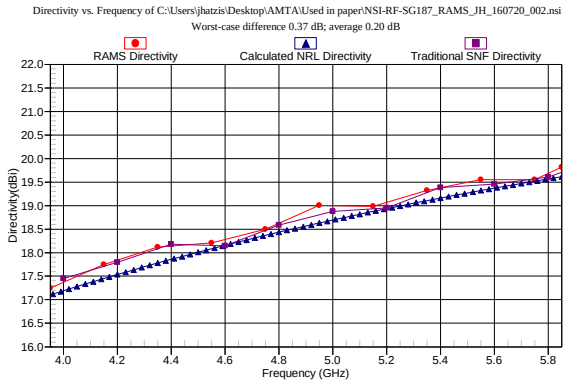

Figure 21. Comparison of directivity vs. frequency of θ/ϕ SNF RAMS and of traditional θ/ϕ SNF system

The results shown above do not display perfect agreement and this can be expected, since these results are preliminary and suffer from imperfect RAMS absorber covering and RF cable management. However, it is clear that that the RAMS system provides reliable results. Data also compares favorably between its SNF and PNF configurations as well as with a traditional θ/ϕ SNF system. The effective multi-path level (EMPL) when comparing the RAMS system with a traditional θ/ϕ system was all better than -40 dB. Repeatability of PNF results was excellent, showing an EMPL of -better than -60 dB. Directivity measured with the RAMS SNF compares favorably with both a traditional θ/ϕ system and calculated NRL data with 0.2 dB average error.

While the EMPL values were good, agreement was not perfect. Error sources such as mutual coupling and truncation need to be further investigated in order to quantify their contribution. Nevertheless, the results shown are encouraging, giving the flexibility of this very versatile methodology.

V. Conclusion

A robotic antenna measurement system was developed and investigated. The system is easily reconfigurable to scan in SNF and PNF configurations, though there are important constraints to consider when operating in either configuration. The alignment of RAMS was investigated and good results were achieved. Correction of axes of motion is essential, but with proper implementation the corrected results show excellent performance.

The RAMS was used to measure an antenna in both SNF and PNF configurations, and the results were compared with a traditional θ/ϕ SNF system, showing good agreement.

Further work is needed to refine position correction, in particular radial correction and correction of y position vs. θ angle to address planarity errors. In addition, the performance of the system will be investigated at higher frequencies.

References

[1] D. Novotny, J. Gordon, J. Guerrieri, "Antenna Alignment and Positional Validation of a mmWave Antenna System Using 6D Coordinate Metrology," Proceedings of the Antenna Measurement Techniques Association, November 2014

[2] J. Gordon, D. Novotny, M. Francis, R. Wittmann, M. Butler, J. Guerrieri, "The CROMMA Facility at NIST Boulder: A Unified Coordinated Metrology Space for Millimeter-Wave Antenna Characterization," Proceedings of the Antenna Measurement Techniques Association (AMTA), November 2014

[3] J. Guerrieri, J. Gordon, D. Novotny, M. Francis, R. Wittmann, M. Butler, "Configurable Robotic Millimeter-Wave Antenna Facility," 9th European Conference on Antennas and Propagation (EuCAP), May 2015

[4] D. Novotny, M. Francis, R. Wittmann, J. Gordon, J. Guerrieri, A. Curtin, "Multi-purpose Configurable Range for Antenna Testing Up To 220 GHz," 10th European Conference on Antennas and Propagation (EuCAP), April 2016

[5] D. Novotny, J. Gordon, M. Francis, R. Wittmann, A. Cutrin, J. Guerrieri, "Antenna Measurement Implementations and Dynamic Positional Validation Using a Six Axis Robot," Proceedings of the Antenna Measurement Techniques Association (AMTA), October 2015

[6] C. Parini, S. Gregson, J. McCormick and D.J. van Rensburg, Theory and Practice of Modern Antenna Range Measurements. London, UK: The Institute of Engineering and Technology, 2015.

[7] G. Hindman, P. Pelland and G. Masters, "Spherical geometry selection used for error evaluation", in the proceedings of the 37th annual AMTA meeting and symposium, Long Beach, CA, USA, 2015.

[8] G. Hindman and A.C. Newell, "Spherical near-field self-comparison measurements", in the proceedings of the 26th annual AMTA meeting and symposium, Atlanta, GA, USA, 2004.

[9] A.C. Newell and G. Hindman, "Antenna pattern comparison using pattern subtraction and statistical analysis", The 5th European Conference on Antennas and Propagation (EuCap), Rome, Italy, 2011.